INTERNATIONAL JOURNAL FOR NUMERICAL METHODS IN FLUIDS
Int. J. Numer. Meth. Fluids 2001; **35**: 199–219

High order schemes for the scalar transport equation

J. A. Hernández*,[1]

Dpto. de Matemática Aplicada y Estadística, E.T.S.I. Aeronáuticos, Universidad Politécnica de Madrid, Plaza Cardenal Cisneros 3, 28040 Madrid, Spain

SUMMARY

A finite volume hybrid scheme for the spatial discretization that combines a fixed stencil and a stencil determined by the classical essentially non-oscillatory (ENO) scheme is presented. Evolution equations are obtained for the mean values of each cell by means of piecewise interpolation. Time discretization is accomplished by a classical fourth-order Runge–Kutta. Interpolation polynomials are determined using information of adjacent cells. While smooth regions are interpolated by means of a fixed molecule, discontinuous or sharp regions are interpolated by the classical ENO algorithm. The algorithm estimates the interpolation error at each time step by means of two interpolants of order q and $q+1$. The main computational load of the resultant scheme is in the interpolation, which is performed by the divided differences table. This table involves $O(qN)$ operations, where q is the interpolation order and N is the number of cells. Finally, linear test cases of continuous and discontinuous initial conditions are integrated to see the goodness of the hybrid scheme. It is well known that, for some particular initial conditions, the classical ENO scheme does not perform properly, not attaining the truncation error of the scheme. It is shown that, for the smooth initial condition, $\sin^4(x)$, the classical ENO scheme does not preserve the character of stability of the initial value problem, giving rise to unstable eigenvalues. The proposed hybrid scheme solves this problem, choosing a fixed stencil over the whole computational domain. The resultant schemes are equivalent to the classical finite difference schemes, which preserve the character of stability. It is also known that the same degeneracy of the error can be encountered for discontinuous solutions. It is shown for the initial discontinuous solution, e^{-x}, that the classical ENO algorithm does not perform properly due to the conflict between the selection of the stencil to smoother regions (downwind region) and the hyperbolic character of the problem, which obliges us to take information from downwind. The proposed hybrid scheme solves this problem by choosing a fixed stencil over the whole computational domain except at the discontinuity. Copyright © 2001 John Wiley & Sons, Ltd.

KEY WORDS: ENO; finite difference; finite volume; high-order scheme; interpolant polynomials; one-dimensional transport equation

* Correspondence to: Dpto. de Matemática Aplicada y Estadística, E.T.S.I. Aeronáuticos, Universidad Politécnica de Madrid, Plaza Cardenal Cisneros 3, 28040 Madrid, Spain. Tel.: + 34 91 3366326; fax: + 34 91 3366324.
[1] E-mail: juan@dmae.upm.es

Received July 1999
Revised January 2000

1. INTRODUCTION

The study of problems where discontinuous solutions are expected requires a special class of algorithm in order not to obtain spurious oscillations. Spectral methods have been adapted by the use of filtering to inhibit oscillations. Harten *et al.* [1] developed finite difference, essentially non-oscillatory (ENO) algorithms to eliminate spurious oscillations near discontinuous solutions, choosing an adaptive scheme oriented to the smoothest region of the solution. However, it was shown by Rogerson and Meiburg [2] that for some particular initial value problems, the classical ENO algorithm presents an accuracy degeneracy. They suggested that these accuracy problems were due to unstable stencils elected by the classical ENO scheme. Shu [3] proposed a modified ENO scheme in order to avoid the anomalous behavior of the error of classical ENO schemes.

Liu *et al.* [4] introduced a new version of ENO that they called weighted essentially non-oscillatory (WENO). They proposed to use a convex combination of all possible stencils to achieve the ENO property, and showed how the WENO schemes have one order of improvement in accuracy and do not suffer the error degeneracy. In their work, the weights of each stencil are obtained by an indicator of smoothness. Jiang and Shu [5] improved the high-order WENO schemes by means of a new way of measuring the smoothness of a numerical solution.

Harten [6] proposed a multi-resolution scheme based on a set of nested grids, which uses a standard centered scheme in all regions but those where a discontinuity is identified, in which case an ENO scheme is used. The way he identifies the discontinuity is based on different grids. Adams and Shariff [7] proposed a hybrid compact-ENO finite difference scheme for simulation of fluid convection problems analyzing their resolution properties and their numerical stabilities. The algorithm they used to identify regions where it is necessary to switch to the ENO scheme is based on the gradient of the solution. Bauer [8] described a hybrid adaptive-ENO scheme, which combines finite difference approximations for points away from the shock and ENO approximations near the shock. In his work, the local truncation error is used to add or to eliminate grid points and to decide when the ENO selection should be used.

In this paper, a high-order spatial discretization is presented to solve the scalar transport equation

$$\frac{\partial w}{\partial t} + c\frac{\partial w}{\partial x} = 0 \tag{1.1}$$

where $w(x, t)$ is a scalar that is transported at constant velocity c. We consider the initial value problem (1.1) with $w(x, 0) = w^0(x)$ and periodic boundary conditions in the compact domain $[-\pi, \pi]$. We discretize the interval $[-\pi, \pi]$ with $N+1$ frontiers $\{x_j,\ j = 0, \ldots, N\}$. So, we have N cells or control volumes $[x_{j-1}, x_j]$ of constant size $\Delta x = x_j - x_{j-1}$. Integrating Equation (1.1) in each cell, we obtain the following finite volume formulation:

$$\frac{\partial}{\partial t}\int_{x_{j-1}}^{x_j} w\ \mathrm{d}x + c[w(x_j, t) - w(x_{j-1}, t)] = 0 \tag{1.2}$$

where $cw(x_j, t)$ and $cw(x_{j-1}, t)$ are the fluxes of the scalar $w(x, t)$ through the frontiers of cell j. Applying the mean value theorem to Equation (1.2), we obtain an ordinary differential equation (ODE) system for the mean values $\tilde{w}_j$

$$\frac{d\tilde{w}_j}{dt} + \frac{c}{\Delta x}[w(x_j, t) - w(x_{j-1}, t)] = 0, \quad j = 0, \ldots, N \tag{1.3}$$

Since the solution of Equation (1.1) is the initial condition travelling at constant velocity c, the fluxes at the frontiers x_j and x_{j-1} are obtained from the solution to the right or to the left of the frontiers depending on the sign of c. The next step is to determine the interpolated solution at the frontiers $w(x_j, t)$, $w(x_{j-1}, t)$ as a function of mean values $\bar{w}_j$.

The motivation of our work is twofold. First, to develop an efficient and easy to implement hybrid scheme (fixed stencil–ENO stencil) of high-order resolution for the spatial discretization. Second, to develop a scheme that does not permit the selection of the stencil by the ENO algorithm in regions where the solution is smooth. This second characteristic is motivated by the anomalous behavior of error for some initial value problems integrated by the classical ENO scheme. The prefixed stencil will permit us to preserve the character of stability of the differential equation and to assure the numerical stability of the round-off error. Even though the present work has been confined to constant step size Δx, no modifications are needed in the algorithm to obtain the scheme for unevenly spaced frontiers.

In Section 2, interpolation by mean values $\bar{w}_j$ is performed by analyzing the computational cost and an estimate for the interpolation error is given based on two interpolants of orders q and $q+1$. In Section 3 we obtain the well-known linear system of equations that governs the evolution of the spatial error, identifying the source of the truncation error and the connection between stability and error. In Section 4 an algorithm is given to choose the stencil used in the interpolation at each control volume. Fixed stencil for every interpolant is considered over the whole computational domain unless the estimation of the interpolation error given in Section 2 is greater than the average error. Section 5 presents for the scalar transport equation the equivalence between classical finite difference schemes and schemes obtained with a fixed stencil for the interpolants. Since the resultant space discretization has a matrix that is function of space and time, in Section 6 we discuss the hypothesis of the frozen argument of the matrix to analyze the stability of the system by means of eigenvalues of stability. Finally, in Section 7 we integrate two different initial conditions: continuous and discontinuous. In Section 7.1 we consider the initial condition $\sin^4(x)$, showing the eigenvalues of the finite difference spatial operator obtained with the classical ENO scheme. We notice that for smooth function, the proposed hybrid scheme gives rise to a classical finite difference scheme, and thus it avoids spurious unstable eigenvalues. In Section 7.2 we consider the initial condition e^{-x} with a discontinuity at $x = 0$ as an example in which the ENO algorithm enters in conflict with the upwind character of the problem. We also show how the proposed hybrid scheme will only change the prefixed stencil for the interpolants near the discontinuity giving rise to numerical solutions much better resolved than those obtained by a classical ENO scheme.

2. PIECEWISE POLYNOMIAL INTERPOLATION

The order of scheme (1.3) is determined by the approximate fluxes obtained from the interpolations at each cells. Hence, the error of the interpolation gives the truncation error of the scheme. We look for a polynomial in each cell using information of the neighboring cells. We notice that the interpolation is completely independent from the problem itself. Therefore, the best interpolations for smooth functions are spectral methods, such as Fourier, Chebyshev or Legendre. The spectral accuracy of these methods gives rise to convergence behavior faster than any interpolating polynomial (Canuto *et al.* [9]). However, the use of Fourier series to interpolate functions with discontinuities causes a very slow convergence and oscillations at both sides of each jump, called Gibbs's phenomenon. There is no uniform convergence to the function, but in L_2. Besides, periodic boundary conditions should be imposed to have spectral accuracy. This motivates the use of piecewise interpolant polynomials. Hence, when the solution is expected to be discontinuous or the boundary conditions are not periodic, interpolation by means of piecewise polynomials is useful. For each cell j and each variable we can define the interpolation polynomial of order q

$$I_j(x, q) = a_0 + a_1 x + a_2 x^2 + \cdots + a_q x^q \tag{2.1}$$

We need $q+1$ conditions to get the coefficients $(a_0, a_1, \ldots, a_q)$. Imposing that the interpolation verifies the mean value $\bar{w}_i$ for s control volumes $[x_{i-1}, x_i]$ to the left of j and $q-s$ mean values to the right

$$\bar{w}_i = a_0 + \frac{a_1}{2\Delta x_i}(x_i^2 - x_{i-1}^2) + \cdots + \frac{a_q}{(q+1)\Delta x_i}(x_i^{q+1} - x_{i-1}^{q+1}), \quad i = j-s, \ldots, j+q-s \tag{2.2}$$

we obtain a linear system of $q+1$ equations and unknowns. Since the matrix of system (2.2) does not have any special property, the solution of (2.2) involves $O(q^2)$ operations. Harten [1] proposed a method that involves only $O(q)$ operations. The idea is to use a primitive function

$$U(x, t) = \int_0^x w(\eta, t)\, \mathrm{d}\eta \tag{2.3}$$

for which the exact value at the frontiers x_j is known

$$U(x_j, t) = \sum_{i=0}^{j} \Delta x_i \bar{w}_i, \quad j = 0, \ldots, N \tag{2.4}$$

It permits us to obtain an interpolation polynomial $H_j(x, q+1)$ for $U(x, t)$ at each control volume j by means of $q+2$ frontiers $\{x_i, i = j-s-1, \ldots, j+q-s\}$, where the value of the primitive function $U(x_i, t)$ is known (see Figure 1). In this case, the matrix of the resultant system is of the Vandermonde type. Hence, the system can be solved by means of the divided difference algorithm (Lambert [10]), which involves $O(qN)$ operations. The interpolant polynomial $H_j(x, q+1)$ is expressed as

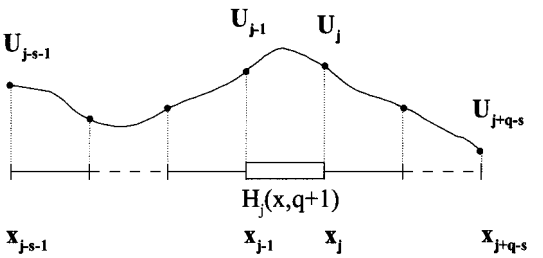

Figure 1. Interpolation polynomial $H(x, q+1)$ of the primitive function $U(x, t)$ for the control volume $[x_{j-1}, x_j]$.

$$H_j(x, q+1) = \sum_{i=0}^{q} c_i L_i(x), \quad L_i(x) = (x - x_{j-s})(x - x_{j-s+1}) \cdots (x - x_{j-s+i-1}) \tag{2.5}$$

where the coefficients c_i are obtained from the divided difference table. Since $H_j(x, q+1)$ interpolates a primitive of $w(x, t)$, we derive Equation (2.5) to obtain the interpolation polynomial of $w(x, t)$

$$I_j(x, q) = \sum_{i=1}^{q} c_i \frac{\mathrm{d}L_i}{\mathrm{d}x} \tag{2.6}$$

where

$$\frac{\mathrm{d}L_i}{\mathrm{d}x} = \frac{\mathrm{d}L_{i-1}}{\mathrm{d}x}(x - x_{j-s+i-1}) + L_{i-1}, \quad i = 1, \ldots, q \tag{2.7}$$

It is important to note that the interpolation $I_j(x, q)$ verifies the mean value theorem for the control volume j

$$\frac{1}{\Delta x_j} \int_{x_j}^{x_{j+1}} I_j(x, q)\, \mathrm{d}x = \frac{1}{\Delta x_j} [H_j(x_{j+1}, q+1) - H_j(x_j, q+1)] = \bar{w}_j \tag{2.8}$$

so that the expression given by Equation (2.6) coincides with the interpolation polynomial given by Equation (2.1). Besides, the main computational load is the construction of the divided difference table, which involves $O(qN)$ operations.

It is well known that for smooth functions ($w(x, t) \in \mathscr{C}^{q+1}$), the interpolation error ϵ_j, defined as the difference between the interpolated value and the exact value at the frontier x_j, can be expressed as

$$\epsilon_j = k_{q+1} w_j^{(q+1)} \Delta x^{q+1} + O(\Delta x^{q+2}) \tag{2.9}$$

where $w_j^{(q+1)}$ is the derivative of order $q+1$ evaluated at frontier x_j and k_{q+1} is a constant that depends on the stencil. If jumps or discontinuities are located at the frontiers of the cells, the interpolation error is also $O(\Delta x^{q+1})$. However, if jumps are between two frontiers, interpolation error is $O(1)$ (Abgrall [11]).

In order to estimate the interpolation error we construct two interpolants with a fixed stencil given by s of orders q and $q+1$. Taking into account the asymptotic expansion of Equation (2.9), we can estimate the interpolated errors to the left (E_j^{L}) and to the right (E_j^{R}) of frontier x_j

$$E_j^{\mathrm{L}} = I_j(x_j, q+1) - I_j(x_j, q), \qquad E_j^{\mathrm{R}} = I_{j+1}(x_j, q+1) - I_{j+1}(x_j, q) \tag{2.10}$$

For smooth functions, the above estimations behave asymptotically as the interpolation errors (2.9). For discontinuous or sharp functions, these estimations will flag the presence of great interpolation errors.

3. ERROR OF THE SPATIAL DISCRETIZATION

We consider the finite volume formulation (1.3) with velocity $c=1$. The exact solution is this initial condition travelling to the right at constant velocity $c=1$ and, hence, the values of $w(x_j, t)$ and $w(x_{j-1}, t)$ in Equation (1.3) are approximated by the values of the interpolant polynomials to the left of the frontiers x_j and x_{j-1} respectively

$$\frac{\mathrm{d}\bar{w}_j}{\mathrm{d}t} = -\frac{1}{\Delta x}\left[I_j(x_j, q) - I_{j-1}(x_{j-1}, q)\right] \tag{3.1}$$

where $\bar{w}_j$ is the approximate mean value of the solution at cell j. Since the interpolations are built with mean values $\{\bar{w}_i,\ i=1,\ldots,N\}$, the right-hand side of Equation (3.1) can be approximated by means of a linear difference operator

$$\frac{\mathrm{d}\bar{w}_j}{\mathrm{d}t} = \sum_{k=1}^{N} L_{jk}\bar{w}_k \tag{3.2}$$

where L_{jk} is the matrix of the system.

In order to discuss the differences between the spatial error and the truncation error of the discretization, we define the error of the spatial discretization at each control volume as the difference between the exact mean value and the approximate mean value

$$\bar{E}_j(t) = \tilde{w}_j(t) - \bar{w}_j(t) \tag{3.3}$$

If we combine Equations (1.3) and (3.2), we obtain the following differential equation for the error at each control volume:

$$\frac{d\bar{E}_j}{dt} = \sum_{k=0}^{N} L_{jk}\bar{E}_k + T_j \tag{3.4}$$

where $T_j(t)$ is the truncation error of the spatial discretization

$$T_j(t) = \frac{1}{\Delta x}\left[I^e_{j-1}(x_{j-1}, q) - w(x_{j-1}, t) - I^e_j(x_j, q) + w(x_j, t)\right] \tag{3.5}$$

In the above expression, $I^e_j(x_j, t)$ represents the interpolated value at frontier x_j obtained from the exact mean values $\tilde{w}_j(t)$, which is different to the interpolated value at frontier x_j appearing in Equation (3.1) obtained from the approximate mean value $\bar{w}_j(t)$.

If the solution is smooth ($w(x, t) \in \mathscr{C}^{q+1}$), then the interpolation error can be expressed using Equation (2.9) as

$$I^e_j(x_j, q) - w(x_j, t) = k_{q+1} w^{(q+1)}_j \Delta x^{q+1} + O(\Delta x^{q+2}) \tag{3.6}$$

where the value of the constant k_{q+1} depends on the stencil used for the interpolation. So, the truncation error (3.5) can be expressed as

$$T_j = (k^1_{q+1} w^{(q+1)}_j - k^2_{q+1} w^{(q+1)}_{j-1})\Delta x^q + O(\Delta x^{q+1}) \tag{3.7}$$

The order of the truncation error (3.7) is, in general, $O(\Delta x^q)$, but if the same computational molecule is chosen for the two interpolants $I^e_j(x, q)$ and $I^e_{j-1}(x, q)$, then k^1_{q+1} coincides with k^2_{q+1} and the truncation error (3.7) is $O(\Delta x^{q+1})$. On the contrary, if two different stencils are used for the two interpolants of (3.1), one order is lost and the truncation error is $O(\Delta x^q)$.

Even though the truncation error was small, the error of the spatial discretization may grow, not behaving asymptotically as the truncation error does. Rogerson and Meiburg [2] and Shu [3] reported this phenomena for $w^0(x) = \sin^4(x)$ and $w^0(x) = e^{-x}$ as the initial conditions. They argued that some stencils of the interpolants give rise to instabilities, which could make loose the accuracy of the scheme. Since the behavior of the spatial error is given by system (3.4), the matrix L_{jk} determines the stability of the error. To secure the acuracy of the scheme, we need an algorithm to elect between all the possible stencils of the interpolants of Equation (3.1), in order to determine the variable computational molecule and, consequently, the matrix L_{jk}.

In the next section we will propose an algorithm to elect the stencil that gives rise to hybrid schemes between classical finite difference schemes and classical ENO schemes.

4. ALGORITHM TO CHOOSE THE STENCIL

Once we have a low-cost method to interpolate the solution in each cell j with order q, we need an algorithm to choose the control volumes of (2.2).

Harten *et al.* [1] developed an ENO algorithm in order to obtain the computational molecule. This algorithm consist of choosing the smoothest polynomial. The information of two cells is needed for the linear reconstruction, and so there are two possible polynomials

depending on whether the left or the right cell is used. The ENO algorithm chooses the one whose slope is the lower in absolute values ($|a_1|$ minimum, see Equation (2.1)). Then, we add both a right cell and a left cell and the ENO algorithm chooses the cell which minimizes $|a_2|$. We proceed this way for higher orders, a cell to the right and another to the left are added to the q order and the cell which minimizes $|a_q|$ is chosen. This algorithm works very efficiently for discontinuous functions. If a discontinuous function must be interpolated, the ENO algorithm takes information from control volumes opposite to the discontinuity, avoiding the oscillating Gibbs phenomenon. However, for particular problems (Shu [3]), the ENO algorithm performs poorly. This motivates the use of a different algorithm to choose the stencil of the interpolants.

In this paper, we develop a hybrid scheme similar to those described in Harten [6], Adams and Shariff [7] and Bauer [8] to get an interpolation polynomial with a fixed stencil for smooth regions and with a stencil determined by the original ENO algorithm for discontinuous or sharp regions. The first step of this algorithm is to identify the regions where the function is sharp or discontinuous, which correspond to the great error of the interpolation. We use the estimations given in Section 2 for the interpolation error to identify the sharp or discontinuous regions and as we notice in the expressions (2.10), the interpolants are built from the approximate mean values w_j of Equation (3.2). The ENO algorithm is used for control volumes that verify the interpolation error to the right or to the left of their frontiers, x_{j-1} and x_j, were greater than a specific value of the L_2-norm of the interpolation error

$$E_j^{\mathrm{R}} > \beta L_2^{\mathrm{R}} \quad \text{or} \quad E_{j-1}^{\mathrm{L}} > \beta L_2^{\mathrm{L}} \tag{4.1}$$

where β is an adjustable parameter and L_2^{R} and L_2^{L} are defined by

$$L_2^{\mathrm{R}} = \sqrt{\frac{1}{N}\sum_{j=0}^{N}(E_j^{\mathrm{R}})^2}, \qquad L_2^{\mathrm{L}} = \sqrt{\frac{1}{N}\sum_{j=0}^{N}(E_j^{\mathrm{L}})^2} \tag{4.2}$$

By this way, to determine the fluxes at each cell interface, five steps must be accomplished: (i) construction of the divided difference tables from the mean values $\bar{w}_j$, which involves $O(qN)$ operations; (ii) interpolation of order q at cell interfaces given by Equation (2.6) with a fixed stencil, which involves $O(qN)$ operations; (iii) interpolation of order $q+1$ in order to estimate the interpolation error by means of Equation (2.10), which involves $O(N)$ operations; (iv) selection of the stencil by the ENO algorithm for control volumes that have a frontier, which verifies Equation (4.1); and (v) interpolation of solution at cell interfaces, which belong to control volumes identified in step (iv). The computational cost of this algorithm has an insignificant increment with respect to a classical ENO algorithm.

It is important to notice that this hybrid scheme has a degree of freedom: the real parameter β. If $\beta = 0$, the resultant scheme is a classical ENO scheme, since condition (4.1) is verified in every control volume. If $\beta \to \infty$, the resultant scheme has a fixed stencil for the interpolants of every control volume and we will show in Section 5 that these schemes are equivalent to the classical finite difference schemes. In between, $\beta \in (0, +\infty)$, the resultant scheme is the mentioned hybrid between finite difference and classical ENO schemes.

For smooth functions, finite difference schemes perform properly and there is no reason to change the prefixed stencil of the interpolant. Thus, a value of β great enough will not permit to change the stencil. If derivatives of the function are of order unity this condition is fulfilled with β of order unity. For discontinuous functions, it is useful to change the stencil according to the ENO algorithm in places where the function has a jump or a discontinuity. If we suppose that the function has only one jump of order unity over the whole computational domain, the L_2-norm of the interpolation error given by Equation (4.2) is $O(\Delta x^{1/2})$. In smooth regions, where the interpolation error is small $O(\Delta x^{q+1})$, the stencil should remain unchanged. This limits the minimum value of β to $O(\Delta x^{q+1/2})$. Since the ENO algorithm should enter to change the interpolation stencil in discontinuous regions, condition (4.1) should be verified limiting the maximum value of β to $O(\Delta x^{-1/2})$. For those discontinuous solutions, where ENO performs poorly, β can be optimized to minimize spurious oscillations of classical finite difference schemes.

5. SCHEMES WITH A FIXED STENCIL

The aim of this section is to show the equivalence between finite difference schemes at some collocation points and high-order schemes (3.2) obtained by interpolants with a fixed stencil over the whole computational domain. If the function to interpolate is smooth enough, the algorithm described in Section 4 chooses a fixed stencil for every computational molecule and, consequently, elements of L_{jk} are constant in time and the truncation error (3.7) is of order $q+1$, as we have seen in Section 3.

We consider the differential formulation (1.1) with $c=1$ integrated along x

$$\frac{\partial U}{\partial t}+\frac{\partial U}{\partial x}=w(0,t) \tag{5.1}$$

where $U(x,t)$ is the primitive of $w(x,t)$. If we verify the differential formulation (5.1) at the collocation points given by the frontiers $\{x_j,\ j=0,\ldots,N\}$, we obtain

$$\left(\frac{\partial U}{\partial t}\right)_{x_j}+\left(\frac{\partial U}{\partial x}\right)_{x_j}=w(0,t),\quad j=0,\ldots,N \tag{5.2}$$

The spatial differential operator of Equation (5.2) can be approximated by means of a finite difference operator involving $q+2$ points, $s+1$ to the left and $q-s$ to the right

$$\left(\frac{\partial U}{\partial x}\right)_j=\frac{1}{\Delta x}\sum_{l=-s-1}^{q-s}\alpha_l U_{j+l} \tag{5.3}$$

where the coefficients α_l are given by the linear system

$$\sum_{l=-s-1}^{q-s}\alpha_l l^s=\delta_{1s},\quad s=0,\ldots,q+1 \tag{5.4}$$

and δ_{ks} is the Kronecker delta. Hence, the spatial discretization of the problem gives rise to the following system of equations:

$$\frac{\mathrm{d}U_j}{\mathrm{d}t} + \frac{1}{\Delta x} \sum_{l=-s-1}^{q-s} \alpha_l U_{j+l} = 0 \tag{5.5}$$

Since $\bar{w}_j \Delta x = U_j - U_{j-1}$, we can obtain a differential equation for $\bar{w}_j$ with Equation (5.5) of the form

$$\frac{\mathrm{d}\bar{w}_j}{\mathrm{d}t} + \frac{1}{\Delta x} \left(\sum_{l=-s-1}^{q-s} \alpha_l \bar{w}_{j+l} \right) = 0 \tag{5.6}$$

We now proceed to obtain an equation for the spatial error $\bar{E}_j$ defined by Equation (3.3). We define the spatial error of the primitive function at each frontier as

$$D_j = U(x_j, t) - U_j(t) \tag{5.7}$$

where $U(x_j, t)$ is the exact value of the primitive function at frontier x_j. If we combine Equations (5.2) and (5.5), we can obtain the evolution equation of D_j

$$\frac{\mathrm{d}D_j}{\mathrm{d}t} + \sum_{l=-s-1}^{q-s} \alpha_l D_{j+l} = R_j \tag{5.8}$$

where R_j is the truncation error of the spatial discretization

$$R_j(t) = \left(\frac{\partial U}{\partial x} \right)_{x_j} - \frac{1}{\Delta x} \sum_{l=-s-1}^{q-s} \alpha_l U(x_{j+l}, t) \tag{5.9}$$

If the primitive $U(x, t) \in \mathscr{C}^{q+2}$, the truncation error (5.9) is expressed as

$$R_j = C_{q+2} U_j^{(q+2)} \Delta x^{q+1} + O(\Delta x^{q+2}) \tag{5.10}$$

where C_{q+2} is a constant value given by

$$C_{q+2} = \sum_{l=-s-1}^{q-s} \frac{\alpha_l l^{q+2}}{(q+2)!} \tag{5.11}$$

Since $D_j - D_{j-1} = \bar{E}_j \Delta x$, we can obtain the following evolution equation of the spatial error $\bar{E}_j$:

$$\frac{\mathrm{d}\bar{E}_j}{\mathrm{d}t} + \sum_{l=-s-1}^{q-s} \alpha_l \bar{E}_{j+l} = \tau_j \tag{5.12}$$

where

$$\tau_j(t) = \frac{1}{\Delta x}(R_j - R_{j-1}) \tag{5.13}$$

and, by means of Equation (5.9)

$$\tau_j = C_{q+2} w_j^{(q+2)} \Delta x^{q+1} + O(\Delta x^{q+2}) \tag{5.14}$$

In summary, the truncation error of the finite difference scheme (5.6) with a computational molecule of width $q+2$ is $O(\Delta x^{q+1})$. As we have seen in Section 3, the truncation error of the spatial discretization (3.2) with a fixed stencil for the two interpolants (2.9) is $O(\Delta x^{q+1})$, with a computational molecule of width $q+2$. Since there exists a unique finite difference operator with a truncation error $O(\Delta x^{q+1})$, with a computational molecule of width $q+2$, the system (5.6) coincides with discretization (3.2). Hence, if the interpolation stencil is fixed, the resultant numerical scheme is equivalent to that obtained with a finite difference scheme. It is important to note that there are $q+2$ finite difference schemes of order $O(\Delta x^{q+1})$. However, when the stencil is fixed, formulation (3.2) gives rise to only $q+1$ schemes, which correspond to the computational molecules $\{[\bar{w}_{j-s-1}, \bar{w}_{j+q-s}],\ s=0, \ldots, q\}$ (see Figure 2). The missing scheme has been eliminated by the upwinding character introduced in Equation (3.1). To obtain centered schemes ($s+1=q-s$), the stencil of the interpolant must be $s=(q-1)/2$, which is only possible if the order q of the polynomial interpolation is odd. If q is even, all possible schemes are uncentered.

On the other hand, if the stencil for the two interpolants $I_j(x, q)$ and $I_{j-1}(x, q)$ is changed, one order is lost as we have seen in Section 3, and the width of the computational molecule can be in between $q+1$ and $2q+2$. The combinations of the different stencils for the interpolants can give rise to a number of $(q+1)^2$ different schemes along the computational domain.

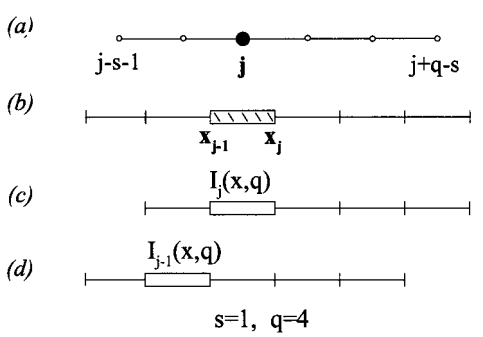

Figure 2. Resultant numerical scheme with interpolant polynomials with fixed stencil. (a) Computational molecule for the mean value $\bar{w}_j$; (b) control volumes involved in the scheme; (c) stencil for the interpolant polynomial for the control volume j; (d) stencil for the interpolant polynomial for the control volume $j-1$.

6. STABILITY OF THE SPATIAL DISCRETIZATION

In this section we compare the stability of the spatial discretization given by Equation (3.2) with the stability of the differential formulation (1.1). The exact solution of (1.1) can be obtained by a Fourier expansion to give

$$w(x, t) = \sum_{k=-\infty}^{k=+\infty} \hat{w}_k^0 \, \mathrm{e}^{\mathrm{i}k(x-t)} \tag{6.1}$$

with

$$\hat{w}_k^0 = \frac{1}{2\pi} \int_0^{2\pi} w^0(x) \, \mathrm{e}^{-\mathrm{i}kx} \, \mathrm{d}x \tag{6.2}$$

Solution (6.1) is a sum of harmonics of different wavenumbers k, which travel at the same constant velocity maintaining their constant amplitude.

The algorithm given in Section 4 chooses the stencil for the interpolants and the system (3.2) is obtained. If the function is smooth, the ENO decision is not necessary and the stencil remains fixed. If the function to interpolate has a great gradient or a discontinuous region, the modified ENO algorithm will shift the stencil to smooth regions. In general, the coefficients L_{jk} are functions of time and the eigenvalues of a frozen L_{jk} make nonsense in the study of stability of disturbances. However, if we consider that the solution $w(x, t)$ is smooth enough, expansion (6.1) is formed with waves of wavelength that are $O(1)$. The numerical scheme will move these waves to the right with a velocity that is $1 + O(\Delta x^q)$, and its amplitude will be reduced or amplified in times that are Δx^{-q} at most. Since the numerical scheme will transport the initial condition maintaining its own amplitude in times $O(1)$, the coefficient matrix L_{jk} can vary only in a long time scale and it makes sense to think of the associated eigenvalues of stability of the frozen matrix.

In cases where the frozen argument makes sense or L_{jk} is constant and if L_{jk} can be diagonalized, fundamental solutions of (3.2) are built with eigenvalues λ_k and eigenvectors $\mathbf{r}_k$ of the frozen matrix L_{jk} and the solution of (3.2) can be expressed

$$\bar{w}_j(t) = d_1 \mathbf{r}_1 \, \mathrm{e}^{\lambda_1 t} + \cdots + d_N \mathbf{r}_N \, \mathrm{e}^{\lambda_N t} \tag{6.3}$$

where $d_1, \ldots, d_N$ are arbitraty constants. It is important that the spatial discretization preserve the character of stability of the differential formulation. Since solution (6.1) is marginally stable, solution (6.3) should be marginally stable, which means that all eigenvalues would have real parts equal to zero ($\mathrm{Re}(\lambda_k) = 0$). Besides, since every harmonic of Equation (6.1) travels at constant velocity, the imaginary part of the eigenvalues divided by k should be unity ($\mathrm{Im}(\lambda_k/k) = 1$). It is well known that when interpolating with piecewise polynomials, the short wavelength is not well integrated, which means that its velocity is different from unity and its amplification factor $\mathrm{Re}(\lambda_k)$ is not equal to zero. A dangerous situation occurs when this short wavelength has $\mathrm{Re}(\lambda_k) > 0$, making these waves unstable and, consequently, the spatial error of the solution growing exponentially.

There are particular cases where the classical ENO algorithm can exhibit problems. If the function is smoother in the downwind direction than in the upwind direction, the classical ENO algorithm will shift the stencil to the downwind direction and the resultant scheme can be unstable. This situation is not so dramatic, since the classical ENO scheme will properly change the stencil in order not to develop the possible instability, but in the meantime the expected order of the ENO scheme is lost. We will show in Section 7 how this situation can be presented for some initial conditions when the stencil is chosen by the classical ENO algorithm. The proposed hybrid algorithm will change the stencil only in regions where the interpolation error is large and will thus avoid the origin of possible unstable schemes.

As an example, we consider a piecewise polynomial interpolation of order $q = 4$. If the stencil is fixed, discretization (3.2) gives rise to five classical finite difference schemes with a computational molecule of width 5, which has a truncation error $O(\Delta x^5)$. In Figure 3(a) we represent the eigenvalues of the linear operator L_{jk} for different stencils fixed to $s = 0, \ldots, 4$ (Figure 3(b)) over the whole computational domain. It is shown how stencils $\{s = 0, 1, 4\}$ have eigenvalues with real parts greater than zero and, consequently, they should be eliminated from the possible candidates of fixed stencil. The hybrid algorithm will fix stencils $s = 2$ or $s = 3$ to integrate Equation (1.1) and will change to other stencils only in sharp or discontinuous regions.

7. NUMERICAL RESULTS AND DISCUSSION

In the following sections we present numerical results for particular initial conditions where the classical ENO algorithm performs poorly. Since we are interested in the spatial discretization,

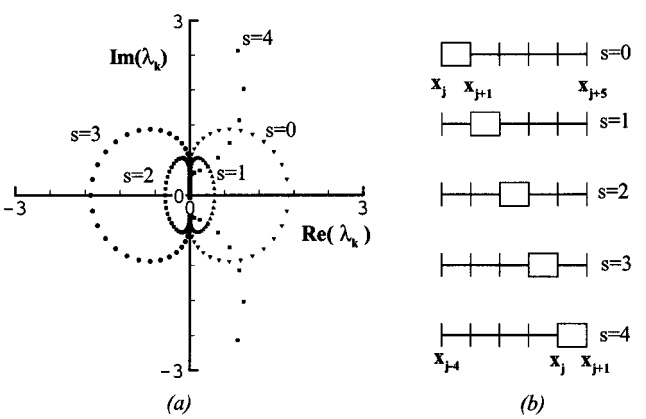

Figure 3. Eigenvalues of the resultant numerical scheme with a fixed stencil. (a) Imaginary part of the eigenvalues versus the real part of a spatial discretized operator obtained with $q = 4$, $N = 50$ and different stencils $s = 0$, 1, 2, 3, 4; (b) possible stencils ($s = 0$, 1, 2, 3, 4) for an interpolant polynomial of fourth-order.

time integration has been accomplished by a classical fourth-order Runge–Kutta. The time step has been chosen in all cases small enough to have time integration errors much smaller than spatial discretization errors.

7.1. Smooth function $w^0(x) = sin^4(x)$

Sometimes the ENO scheme does not deal properly with smooth functions. This is the case of the initial condition $w^0(x) = \sin^4(x)$ reported in the literature [2,3]. It is well known that when the ENO algorithm chooses the stencil, the error does not behave as one could expect. In Figure 4, we represent the L_2-norm of the error at the frontiers to the left (see Equation (4.2)) as a function of time for a classical ENO scheme, with a fourth-order interpolation. It is showed that, for $N \geq 400$, the error grows not maintaining the expected order. The same behavior is shown in Figure 5 for different interpolation orders as a function of the discretization points N. Shu [3] speculated that the error was due to the selection of unstable stencils by the ENO scheme. In the following two figures we represent the initial condition $w^0(x) = \sin^4(x)$, together with the initial stencil chosen by the ENO algorithm for $N = 200$. Once the ENO algorithm chooses the stencil for the smooth initial condition, the smooth solution begins to move to the right at constant velocity. As we have seen in Section 6, numerical diffusion or dispersion will be noticed in long time scales. Thus, the frozen argument for the matrix of the system (3.2) makes sense and the behavior of the error is known from the eigenvalues of stability of L_{jk}. However, the numerical noise (round-off), which is always present, will be amplified if there are eigenvalues with real parts greater than zero. The small characteristic time of this phenomenon is

$$\tau_v = \frac{1}{\sigma_m} \tag{7.1}$$

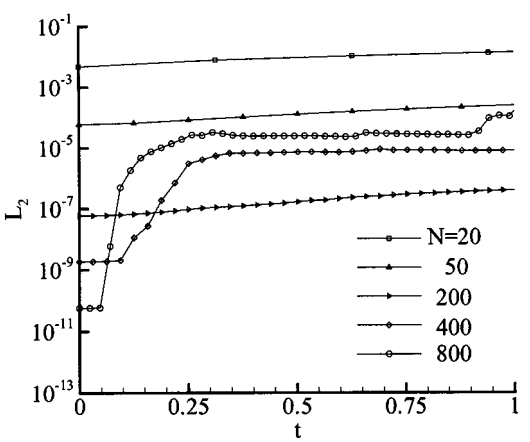

Figure 4. L_2-norm of the error of a classical ENO scheme versus integration time for the initial condition $w^0(x) = \sin^4(x)$, with an interpolation order $q = 4$ and different discretization points N.

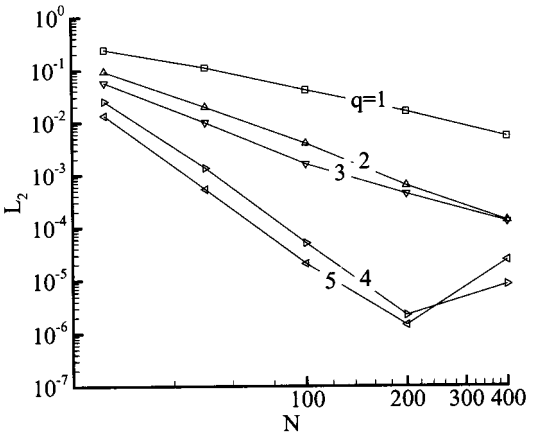

Figure 5. L_2-norm of the error of a classical ENO scheme versus discretization points N for the initial condition $w^0(x) = \sin^4(x)$ and different interpolation orders at time $t = 1$.

where σ_m represents the maximum value of the real part of those eigenvalues with real parts greater than zero. In times $t = O(\tau_v)$, the numerical noise will be amplified and the scheme begins to loose their accuracy. Then, the ENO algorithm will change the stencil so as not to permit the growing of the numerical noise. In summary, even though this situation is not dramatical, it is not desirable.

In Figure 6(a), linear interpolation is considered ($q = 1$) and the ENO algorithm can choose between the stencil $s = 0$ or $s = 1$. In Figure 6(b), the eigenvalues of difference operators have been plotted showing that there are no eigenvalues with real parts greater than zero. In Figure 6(c) and (d) the same initial condition is plotted, but in this case for a second-order interpolation ($q = 2$). It is important to note that now eigenvalues with real parts greater than zero are encountered and, consequently, ENO eventually will change the stencil so as not to have an unstable behavior. In Figure 7 interpolation order $q = 3$ and $q = 4$ are considered. In both cases, eigenvalues with real parts greater than zero appear. These observations allow the conclusion that, for particular initial conditions, the classical ENO algorithm can give rise to finite difference operators with eigenvalues with real parts greater than zero. This fact does not imply that the solution is unstable but that the expected order of the scheme can be lost.

Our hybrid scheme with $\beta = 2$ will always leave the prefixed stencil, as the interpolation error is of the same order of magnitude over the whole computational domain and, thus, the resultant schemes are equivalent to finite difference schemes. In Figure 8 we represent the L_2-norm of the error of the solution at time $t = 2\pi$ for the initial condition $w^0(x) = \sin^4(x)$ versus the discretization points N for different orders. In all cases, the fixed stencil has been chosen by $s = q/2$, which always gives stable eigenvalues. It is shown in Figure 8 that there is no anomalous behavior of the error. The error behaves as expected until the round-off error is achieved. In summary, the hybrid scheme fixes the degeneracy of the error for some particular smooth initial conditions integrating the problem with classical finite difference

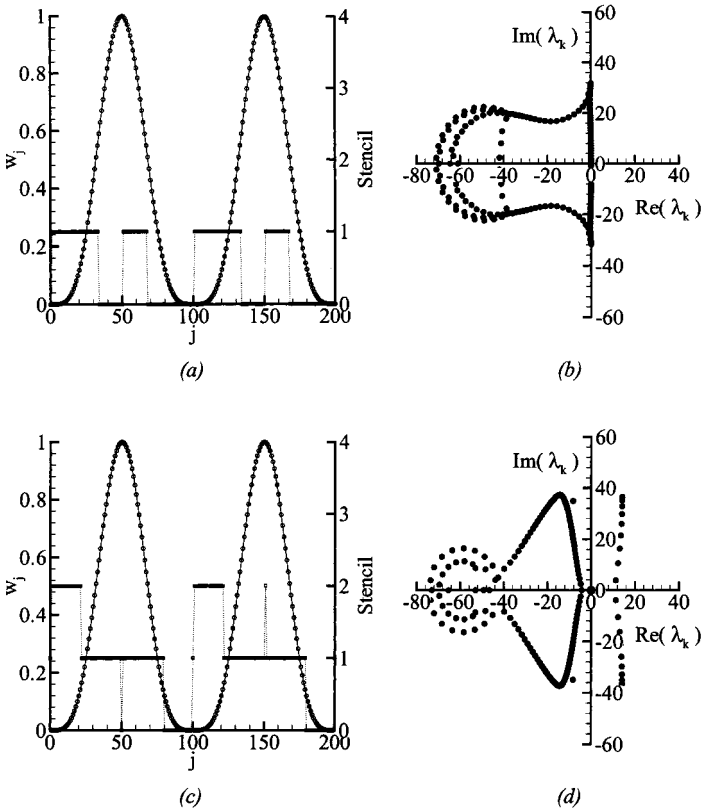

Figure 6. Eigenvalues of the finite difference operator obtained with the classical ENO and the initial smooth condition $w^0(x) = \sin^4(x)$. (a) Initial condition and ENO election of the stencil with linear interpolation; (b) eigenvalues of the resultant numerical scheme with linear interpolation; (c) initial condition and ENO election of the stencil with second-order interpolation; (d) eigenvalues of the resultant numerical scheme with second-order interpolation.

schemes. In the next section we will see the behavior of this algorithm for discontinuous functions.

7.2. Discontinuous function $w^0(x) = e^{-x}$

We consider the initial condition $w^0(x) = \mathrm{e}^{-x}$, which is smoother in the downwind direction. Due to the periodicity of the integration domain, the initial condition has a discontinuity in $x = 0$. This is an example of discontinuous solution where the classical ENO algorithm performs poorly. The reason in this case is different from the preceding case. Since the classical ENO algorithm chooses the stencil that gives the smoothest interpolant polynomial, the resultant scheme for almost every control volume is unstable. In Figure 9 we represent the

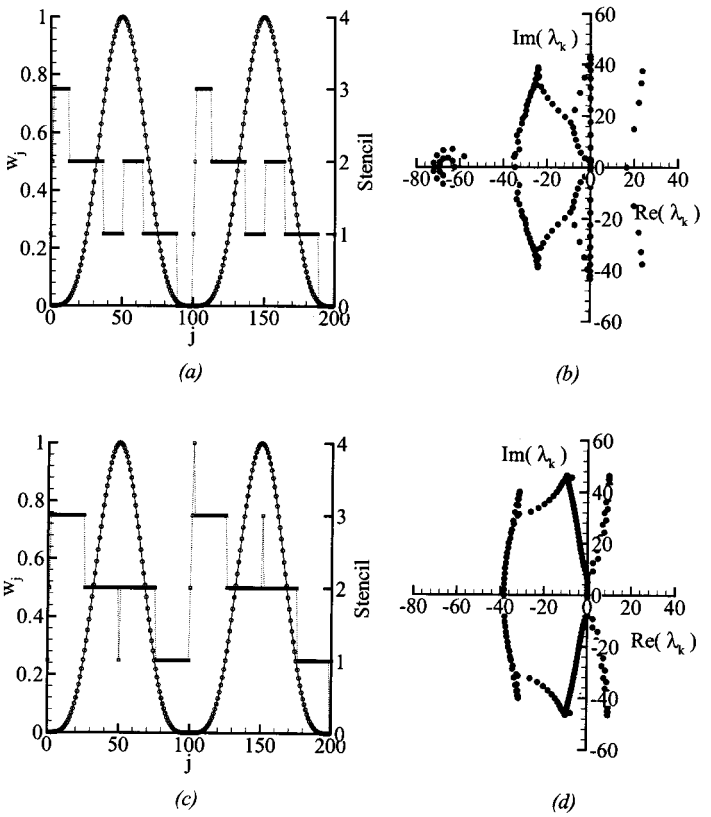

Figure 7. Eigenvalues of the finite difference operator obtained with the classical ENO and the initial smooth condition $w^0(x) = \sin^4(x)$. (a) Initial condition and ENO election of the stencil with third-order interpolation; (b) eigenvalues of the resultant numerical scheme with third-order interpolation; (c) initial condition and ENO election of the stencil with fourth-order interpolation; (d) eigenvalues of the resultant numerical scheme with fourth-order interpolation.

initial condition together with the stencil chosen by the classical ENO algorithm for interpolant polynomial of order $q = 10$. The ENO algorithm chooses the stencil $s = 0$ because the data is smoother upwinding. However, due to the hyperbolic character of the problem, information should be taken from downwind. This controversy between the ENO algorithm and the character of the problem gives rise to an unstable stencil. If this initial selection is maintained along time, the solution becomes unstable. However, with more time, the classical ENO scheme fixes the situation changing the stencil properly. Even though the initial selection does not mean that the solution behaves unstable, this situation is not desirable. In Figure 10 we represent the solution at time $t = 2\pi$. As we can see the solution has not

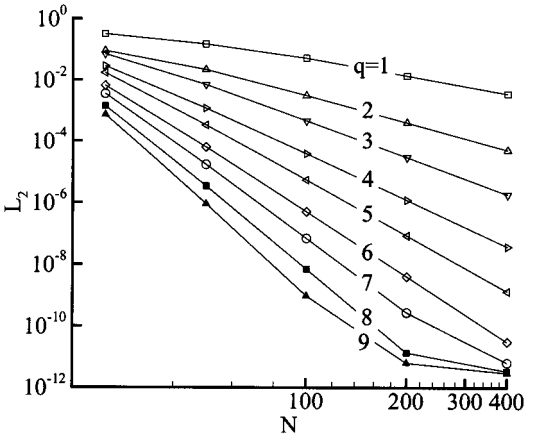

Figure 8. L_2-norm of the error of a modified ENO scheme versus discretization points for the initial condition $w^0(x) = \sin^4(x)$ and different interpolation orders q at time $t = 2\pi$.

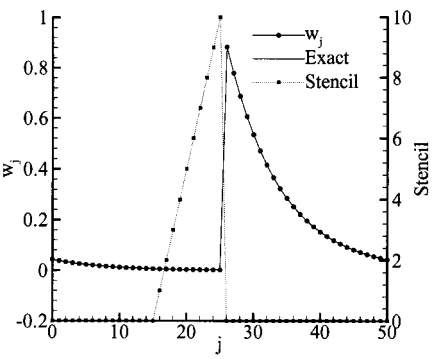

Figure 9. Initial discontinuous condition e^{-x} together with the election of the stencil done by a classical ENO scheme with an interpolation order $q = 10$.

exploded by the possible initial instability but the error is even greater than that obtained with a finite difference scheme (Figure 11). It is well known that, in finite difference schemes, short wavelength is not well resolved and oscillations appear behind the shock. This situation can be solved using the proposed hybrid scheme with $\beta = 1$ as is it shown in Figure 12. The algorithm will change the stencil in regions where the interpolation errors is great. In Figure 13 we represent the solution at time $t = 2\pi$ with 50 control volumes for interpolation orders $q = 0, 1, 4, 10$. Even though the error at the discontinuity is of order unity for every method, high-order methods approximate better than low-order methods.

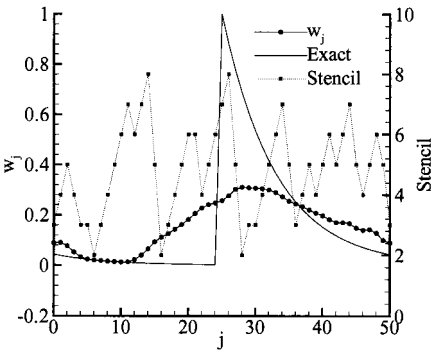

Figure 10. Numerical solution w_j compared with the exact solution at $t = 2\pi$ together with the stencil of a classical ENO scheme with a interpolation order $q = 10$, $\Delta t = 0.00157$ and $N = 50$.

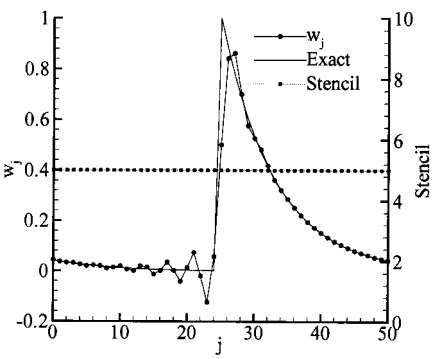

Figure 11. Numerical solution w_j compared with the exact solution at $t = 2\pi$ together with a fixed stencil $s = 5$ of a classical finite difference method with an interpolation order $q = 10$, $\Delta t = 0.00157$ and $N = 50$.

8. CONCLUSIONS

A finite volume hybrid scheme for the spatial discretization that combines a fixed stencil and a stencil determined by classical ENO scheme is proposed. The time discretization is accomplished by a fourth-order Runge–Kutta with a time step small enough to have time errors much less than the spatial errors. The error of the spatial discretized equations for the scalar transport equation is analyzed. The behavior and the stability of the spatial error were investigated for the special initial conditions $w^0(x) = \sin^4(x)$ and $w^0(x) = \mathrm{e}^{-x}$ in the compact domain $[-\pi, \pi]$, with periodic boundary conditions. It is shown how the spatial error is controlled by the truncation error and the stability of a system of differential equations. The stability of the spatial discretization obtained by a original ENO algorithm for the initial condition $w^0(x) = \sin^4(x)$ is investigated and it is shown using the frozen argument of the

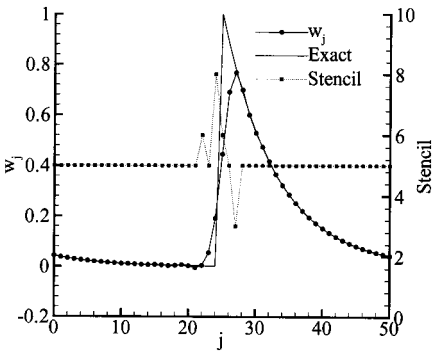

Figure 12. Numerical solution w_j compared with the exact solution at $t = 2\pi$ together with the election of the stencil done by the hybrid scheme with $\beta = 1$, $s = 5$, $q = 10$, $\Delta t = 0.00157$ and $N = 50$.

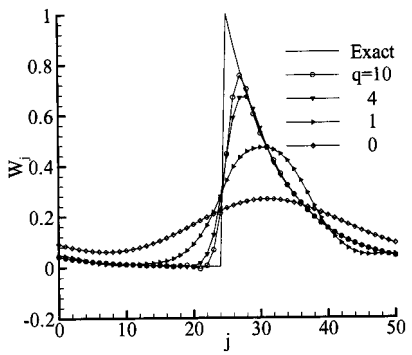

Figure 13. Numerical solutions w_j compared with the exact solution at $t = 2\pi$ integrated with the hybrid scheme with $\Delta t = 0.00157$, $N = 50$, $\beta = 1$, $s = q/2$ and different interpolation orders q.

spatial discretized operator that the system haas unstable eigenvalues for interpolation orders $q \geq 3$. It is also shown that for the initial condition e^{-x}, the classical ENO scheme has a conflict in the selection of the stencil and the hyperbolic character of the problem.

To solve the problem, a hybrid scheme between a finite difference scheme and a classical ENO scheme is proposed. This algorithm identifies regions of the solution that have discontinuities or great gradients by means of two interpolants of orders q and $q + 1$. For the smooth regions a stable fixed stencil for the interpolants is used, showing that the resultant schemes are equivalent to classical finite difference schemes. For sharp regions a classical ENO algorithm enters, modifying the stencil of the interpolants. The numerical experiments show the goodness of the proposed hybrid scheme.

In summary, we could say that our hybrid scheme avoids error degeneracy of classical ENO for those initial conditions in which the upwind character might be in conflict with the ENO

selection of the stencil. For the initial conditions where ENO performs properly, our hybrid scheme performs similar. Extensions for parabolic and non-linear problems are the subject of future works.

REFERENCES

1. Harten A, Engquist B, Osher B, Chakravarthy S. Uniformly high order accurate essentially non-oscillatory schemes III. *Journal of Computational Physics* 1987; **71**: 231–303.
2. Rogerson AM, Meiburg EA. Numerical study of the convergence properties of ENO schemes. *Journal of Science and Computers* 1990; **5**: 151–167.
3. Shu CW. Numerical experiment on the accuracy of ENO and modified ENO schemes. *Journal of Science and Computers* 1990; **5**: 127–149.
4. Liu XD, Osher S, Chan T. Weighted essentially non-oscillatory schemes. *Journal of Computational Physics* 1994; **115**: 200–212.
5. Jiang GS, Shu CW. Efficient implementation of weighted ENO schemes. *Journal of Computational Physics* 1996; **126**: 202–228.
6. Harten A. Adaptive multiresolution schemes for shock computations. *Journal of Computational Physics* 1994; **115**: 319–338.
7. Adams NA, Shariff KA. High-resolution hybrid compact-ENO scheme for shock–turbulence interaction problems. *Journal of Computational Physics* 1996; **127**: 27–51.
8. Bauer RB. A hybrid adaptive ENO scheme. *Journal of Computational Physics* 1997; **136**: 180–196.
9. Canuto C, Hussaini MY, Quarteroni A, Zang TA. *Spectral Methods in Fluid Dynamics*. Springer: Berlin, 1988.
10. Lambert JD. *Numerical Methods for Ordinary Differential Systems. The Initial Value Problem*. Wiley: New York, 1991.
11. Abgrall R. On essentially non-oscillatory schemes on unstructured meshes: analysis and implementation. *Journal of Computational Physics* 1994; **114**: 45–58.

